

CLOSED-LOOP THROTTLE CONTROL OF A N₂O/IPA THRUSTER

BARCELO RENACIMIENTO HOTEL, SEVILLE, SPAIN / 14 - 18 MAY 2018

Iain Waugh^(1,2), Ed Moore⁽¹⁾, and James Macfarlane⁽¹⁾

⁽¹⁾ Airborne Engineering Ltd., Westcott Venture Park, Aylesbury, HP18 0XB, UK

⁽²⁾ Corresponding author: iain@ael.co.uk

KEYWORDS:

VTVL lander, nitrous oxide, throttle control

ABSTRACT:

A project is underway at Airborne Engineering Ltd. (AEL) to develop a VTVL technology demonstrator. A sub-scale vehicle, based on a 300N N₂O /IPA throttleable bipropellant thruster, has been constructed and was presented at the previous conference. This paper presents details of the subsequent throttle control testing, the throttle control system methodology and testing data.

The throttle control of the nitrous oxide was found to be the most difficult element of the thruster control, because the fluid is self-pressurising in the propellant tank and therefore is in a two phase state throughout the plumbing. The mass flow passing through the throttle valve is therefore highly sensitive to the state of the upstream fluid and downstream pressure, because this governs the degree of flash-boiling.

During static testing, two salient points were noted. First, that the N₂O injector pressure drop into the combustion chamber was found to be almost independent of massflow, because of a balance between flash-boiling in the control valve and flash-boiling in the injectors, and second, that the chamber pressure varied almost linearly with the pulse width provided to the N₂O servo control valve. The throttle control system for the N₂O is therefore designed to use feedback control from the combustion chamber pressure, based on a second order transfer function of the thruster response derived from experimental data. The control loops are shown to perform well enough to proceed to vehicle flight testing.

1. INTRODUCTION

There is increasing interest within Europe in carrying out a robotic Lunar or Martian planetary landing mission. This kind of mission requires the development of technologies such as autonomous landing and hazard avoidance. These technologies require testing in a representative environment, such as on a VTVL (vertical take-off, vertical landing) vehicle. VTVL platforms have been developed in the USA, such as the NASA Morpheus project [1, 2] and the Masten Space Systems' Xombie vehicle [3]. These vehicles have been used to successfully demonstrate real-time hazard avoidance as part of the NASA's Autonomous Landing Hazard Avoidance Technology (ALHAT) programme [1, 2, 3]. Such vehicles have been designed to be simple and wherever possible use commercially available components in order to reduce cost [2].

There is a need for access to such a vehicle in Europe for evaluating technologies such as LIDAR instruments and for validating hazard detection and avoidance algorithms. To address this need, a project is underway at Airborne Engineering to develop a VTVL technology demonstrator, in order to develop experience in the design and control of VTVL vehicles. A sub-scale vehicle, based on a 300N isopropyl alcohol (IPA) and nitrous oxide (N₂O) throttleable bipropellant thruster, has been constructed and was presented at the previous conference [4].

Fig. 1 shows the layout of the Gyroc 5 vehicle. It consists of the following primary components: a gimbaled Snark thruster steered by two linear actuators, two pressurised propellant tanks, two low-mass throttle valves and the GNC avionics. The Snark thruster is a variable thrust bipropellant thruster developed by AEL. Snark uses low-hazard propellants and is designed to be easily modifiable and low cost, with the view that it will only be used for short duration firings.

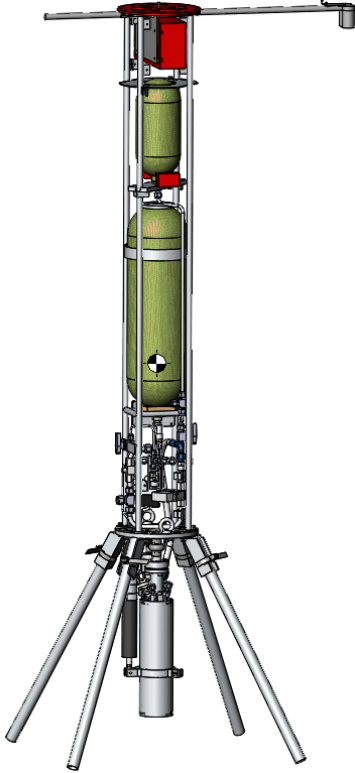


Figure 1: Gyroc 5 VTVL vehicle, configured for flight.

The chamber is constructed from a simple aluminium tube around an ablative canvas phenolic liner of sufficient thickness for several firings; the nozzle is made from graphite with a rounded throat and conical exit.

Nitrous oxide has the advantage that it is self pressurising and therefore does not require a separate pressurant. The isopropyl alcohol is fed from a tank that is pre-pressurised with Nitrogen. Because the tanks are rated to 300bar, the initial pressure can be high and the pressure drop over the short firing duration is acceptable. The IPA throttle control system must take account of this upstream pressure drop, however, in order to maintain the required mass flow.

1.1. Nitrous oxide throttling

Throttle control of nitrous oxide is difficult because the fluid is self-pressurising in the tank and therefore is in a two phase state throughout the plumbing. The mass flow passing through the throttle valve is therefore highly sensitive to the state of the upstream fluid and downstream pressure, because this governs the degree of flash-boiling. Further flash-boiling then occurs during injection into the combustion chamber.

Nitrous oxide flash-boiling in an orifice is a complicated process, which depends on the upstream state, the pressure drop, the stay time in the orifice and the heat load (important for injection into a combustion chamber). It has been studied in detail in the literature [5, 6, 7]. The nitrous oxide behaves somewhere between two limits: first, the single phase incompressible (SPI) limit, where the nitrous oxide remains liquid, and second, the homogeneous equilibrium (HEM) limit, where the nitrous oxide remains in equilibrium, expands isentropically and the phases travel at the same velocity. The model proposed by [6], with a correction by [7] and tested by [5] uses a smooth blending between the SPI and HEM limits, based on the relative bubble growth time and residence time in the injector. This model is known as the Non-Homogeneous Non-Equilibrium (NHNE) model [5], and has been tested extensively for cold flow injection at a range of injector and chamber pressures. The key equations for these are shown below:

$$\dot{m}_{SPI} = C_d A \sqrt{2\rho_1 \Delta p} \quad (1)$$

$$\dot{m}_{HEM} = C_d A \rho_2 \sqrt{2(h_1 - h_2)} \quad (2)$$

$$\dot{m}_{NHNE} = \frac{\kappa}{1 + \kappa} \dot{m}_{SPI} + \frac{1}{1 + \kappa} \dot{m}_{HEM} \quad (3)$$

where

$$\kappa = \sqrt{\frac{p_1 - p_2}{p_v - p_2}}, \quad h_2 = f(p_2, s_1), \quad \rho_2 = f(p_2, s_1) \quad (4)$$

where \dot{m} is the massflow, C_d is the discharge coefficient, A is the area, ρ is the density, h is the specific enthalpy and s is the specific entropy, all in SI units, and κ is the non-equilibrium parameter. Subscripts 1 refers to upstream and 2 downstream of an orifice, and v the saturated vapour limit.

Snark Engine Data (300N Version)	
Fuel	Isopropyl Alcohol
Oxidant	Nitrous Oxide
Throttle range	20%-117%
Nominal full thrust	300N
Measured performance at full thrust:	
Measured c^*	1487m/s
Specific Impulse (sea level)	215s
Oxidiser to Fuel Ratio	5:1
Expansion ratio	1:4.7

Table 1: Data for the Snark bipropellant rocket thruster

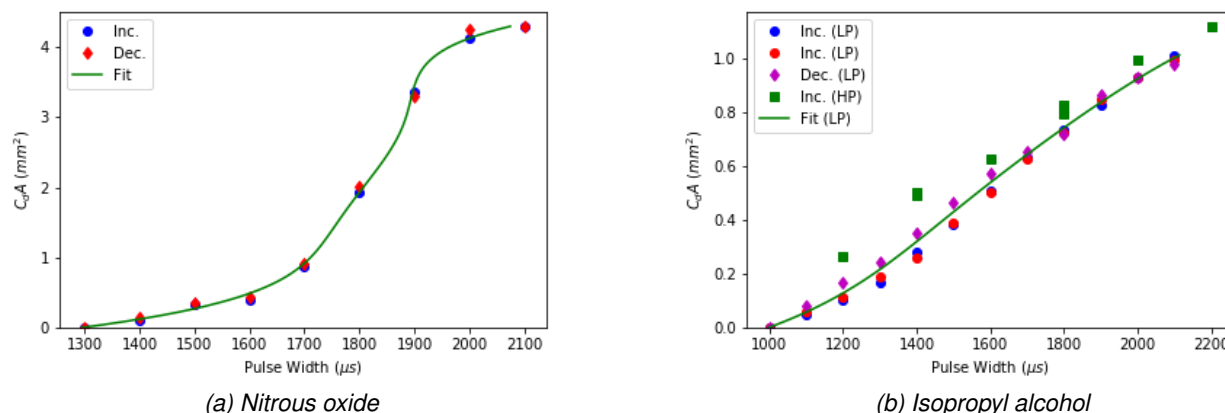


Figure 2: Calibration measurements for the throttle valves, based on the pulse width supplied to the servo motors. There is some hysteresis depending on whether the pulse width is increasing (Inc) or decreasing (Dec). for the IPA valve there is also some horizontal shift between low pressure (LP) test results with water and high pressure (HP) tests with IPA.

Throttling of nitrous oxide has been studied for throttling of hybrid rocket motors using hydroxyl-terminated polybutadiene (HTPB) as a fuel [8, 9, 10]. In these studies the feed system was modelled using the NHNE method to evaluate pressure drops across both the throttle valve (a ball valve) and the injector, and coupled to a chamber pressure correlation in order to design a control loop based on either chamber pressure or thrust feedback. Hot firings demonstrated that the controllers could successfully follow desired profiles with large turndown [9, 10]. A simplification was introduced, however, in that a separate helium supply was used to pressurise the nitrous oxide, such that it was always liquid on entry to the throttle valve and therefore in a known state for input to the NHNE model. In a flight situation, where the nitrous oxide is self-pressurising and the mass flow rate is large compared to the tank volume, the state will in reality be unknown at entry to the throttle valves.

This paper will present details of the Snark thruster throttle control testing and the control system methodology for both the fuel, where the tank pressure drops sharply during testing, and for the nitrous oxide, where flash-boiling occurs in both the throttle valve and the injectors. Performance of the throttle control system is presented with firing data. The thruster control loop and vehicle are shown to perform well and will proceed to flight testing.

2. THROTTLE CONTROL VALVES

Throttling is achieved using modified Swagelok valves actuated with digital servo drives, which are available in compact, flight weight form from the model aircraft industry. Drive shafts were connected with either a rigid coupling (N_2O valve) or a bellows coupling (IPA valve) to allow valve shaft rise. The valves and servos were matched to give sufficient resolution over the required flow range and to provide a positive shut-off. The throttle valves are calibrated to characterise the relationship between pulse width provided to the servo motor and the resulting flow discharge coefficient.

Fig. 2 shows the calibration results for both the N_2O and IPA valves. These results indicate several potential problems. First, that there was a substantial offset in valve opening dependent on the drive direction. This hysteresis was substantially reduced by upgrading the servo to a higher torque model, but it is uncertain whether the improvement was down to torque or the servo's internal control loops, which may contain a deadband. Second, that as shown on the IPA results, there was an offset in opening position dependent on system pressure of roughly $100 \mu s$ between low pressure (LP $\approx 10\text{bar}$) water and high pressure (LP $\approx 75\text{bar}$) IPA results. Third, that in the case of the N_2O valve the correlation is strongly nonlinear.

The first two of these problems mean that it is not possible to simply translate directly between a desired valve opening and the required pulse width. The IPA correlation is almost linear, however, and so is the central section of the N_2O correlation, where the bulk

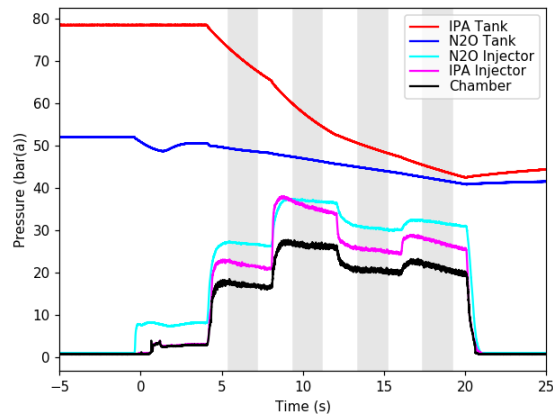


Figure 3: Pressures from open loop testing, where the fuel and oxidiser throttle valves were opened to four preset positions, specified by four pairs of pulse width values. Time-averaging windows are shown as vertical gray bars.

of the throttling occurs. It is therefore possible to extract a gradient value ($\partial C_{dA}/\partial \mu_s$) to estimate the rate of change of valve opening per pulse width, which is used to design the control loops.

3. THRUSTER CHARACTERISATION

The thruster response to throttling will also be governed by several other physical processes, most notably those due to the servo response, filling plumbing volumes in the injectors, and those due to mixing, atomisation and combustion of the propellant. Together these will add a small time delay and will act like a low pass filter, with the exception of any thermoacoustic instabilities, which will act at a much higher frequency than the control loop and can be ignored.

Several hot firings were required to characterise the thruster enough to design the control loops. The initial tests opened both throttles to several predefined positions in terms of pulse width pairs, that were estimated from the valve calibration to maintain the required mixture ratio. Fig. 3 shows example pressure results from one of these tests. Over the first four seconds the engine starts on N_2O alone, before adding a preset quantity of IPA to warm the engine and ensure ignition. Four throttle positions are then specified. In this particular test the resulting mixture ratio was much richer than desired, because a higher IPA tank pressure resulted in an offset in the valve correlation (see

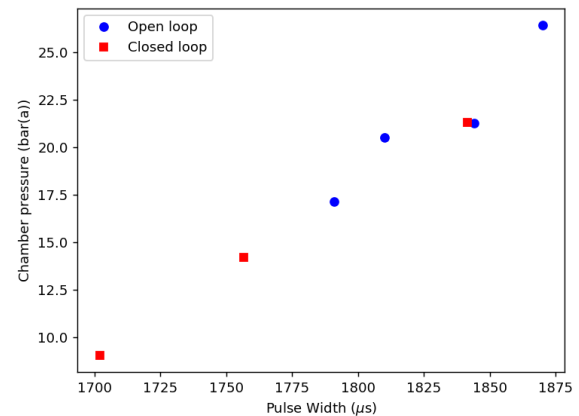


Figure 4: Time-averaged chamber pressures and pulse widths for the N_2O throttle valve, from the open loop testing in Fig. 3 and from the closed loop testing in Fig. 10.

Fig. 2). The four vertical gray bars in Fig. 3 show regions where time-averages can be taken. Note that in each of these regions the chamber pressure decreases because the tank pressures are decreasing and therefore the massflows are decreasing because the valve positions are fixed.

One useful property of the N_2O throttling system was seen during the thruster characterisation process in the linear region of the N_2O throttling valve, where most of the throttling performance is required for vehicle flight. The chamber pressure was found to vary almost linearly with the pulse width supplied to the N_2O servo motor. Fig. 4 shows time averaged results from the open loop testing in Fig. 3, and from the closed loop testing in Fig. 9. The correlation is almost linear, with some small divergence in the open loop testing, which is likely due to variance in the mixture ratio.

Furthermore, it was found that the N_2O injector pressure drop remained almost constant during throttling, which is counterintuitive. Fig. 9 shows the pressure values when throttling at constant mixture ratio. As expected, a lower chamber pressure requires a much lower injector pressure drop for the IPA, because the IPA injector pressure drop is governed by the SPI equation which is proportional to \dot{m}_{IPA}^2 . Figs. 3 and 9 show that the N_2O injector pressure drop, however, is almost constant for all throttle positions.

This data suggests that there is a useful balance between the pressure drops across the N_2O throttle valve and injector. If the valve opening area is reduced, the mass flow across it reduces and therefore

the chamber pressure reduces. The lower chamber pressure results in a higher pressure drop across the throttle valve, and therefore more flash-boiling. The nitrous oxide entering the injector therefore has a lower density and requires a higher pressure drop per unit massflow when compared to a higher throttle setting. The result is that the balance of the flash-boiling in the valve and the injectors gives an almost constant injector pressure drop for the current setup.

4. CONTROL SYSTEM METHODOLOGY

The control methodology for both the IPA and N_2O control loops uses the chamber pressure as a demanded variable. For the Gyroc 5 vehicle, a demanded thrust is the output from the flight position control loops, but this is a difficult variable to measure in a free flight scenario. Given that the chamber pressure is easy to measure accurately, demanded thrust is converted to demanded chamber pressure using a correlation based on the pressure dependent thrust coefficient of the nozzle and the measured throat area (A_t). The chamber pressure, p_c , and thrust, F , can be related to the thrust coefficient, C_F , and characteristic velocity, c^* using:

$$F = C_F A_t p_c = C_F \dot{m}_{TOT} c^* \quad (5)$$

where $C_F = f(\gamma, p_c/p_e, A_e/A_t)$, and the subscript e refers to nozzle exit, t to the throat and c to the chamber. CEA [11] can be used to find $C_F = f(p_c, O/F)$ and $c^* = f(p_c, O/F)$.

Fig. 5 shows the dependence of C_F and c^* on chamber pressure and mixture ratio (O/F). Fig. 5 demonstrates that there is a weak dependence of C_F on O/F, but the difference is less than 0.5% across the range plotted. For real-time estimation of thrust, it is therefore suitable to fit a polynomial to C_F as a function of the logarithm of chamber pressure alone. The logarithm of chamber pressure is used to better capture the sharp dropoff in C_F at low pressures. Fig. 5 also shows that c^* varies by less than 5% over the range of interest. Because c^* will only be used by the control loop for relating a required change in thrust to a change in massflow a small error is acceptable. A polynomial is therefore fitted to the average c^* curve as a function of the logarithm of chamber pressure, and the mixture ratio dependence is neglected. The calculated \dot{m}_{TOT} value can then be split into the required fuel and oxidiser components using a fixed O/F (e.g. 5.0), using:

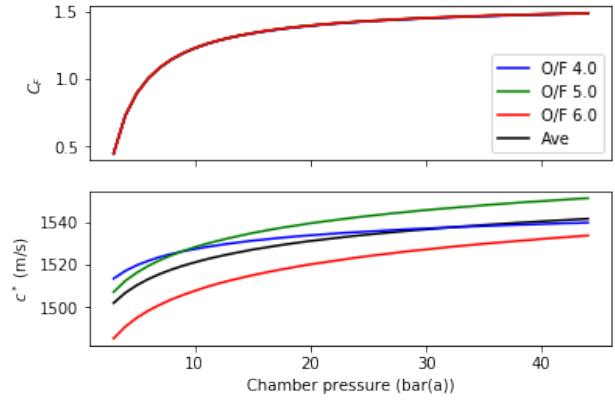


Figure 5: Thrust coefficient, C_F , and characteristic velocity, c^* , as a function of chamber pressure and mixture ratio (O/F), against average curve fits as a function of logarithmic chamber pressure.

$$\dot{m}_{IPA} = \dot{m}_{TOT} \frac{1}{1 + O/F} \quad (6)$$

$$\dot{m}_{N_2O} = \dot{m}_{TOT} \frac{O/F}{1 + O/F} \quad (7)$$

Using these correlations it is therefore possible to convert from a demanded thrust to either a demanded total massflow or a demanded chamber pressure. The first of these conversions will be used for the IPA control loop, which is based on feedback of a massflow related quantity, and the second of these conversions will be used for the N_2O control loop, which is based on feedback from the chamber pressure.

4.1. IPA control system

The IPA throttling process is considerably simpler than for the N_2O , because IPA can be considered to be incompressible and single phase. Fig. 6a shows the model for the basic fuel throttling process, which is split into three steps. First, the conversion from input pulse width to a valve flow area, which uses the linear fit to the correlation in Fig. 2b. Second, the conversion from valve flow area to a massflow, using the SPI equation. Third, the conversion from a massflow to the square root of the injector pressure which can be measured to use as a feedback parameter. This is important, because there is no means of direct massflow measurement on the current flight hardware, only pressure transducers. A massflow measurement device, such as a venturi meter, could be used here instead, but since the injector orifices are a fixed size

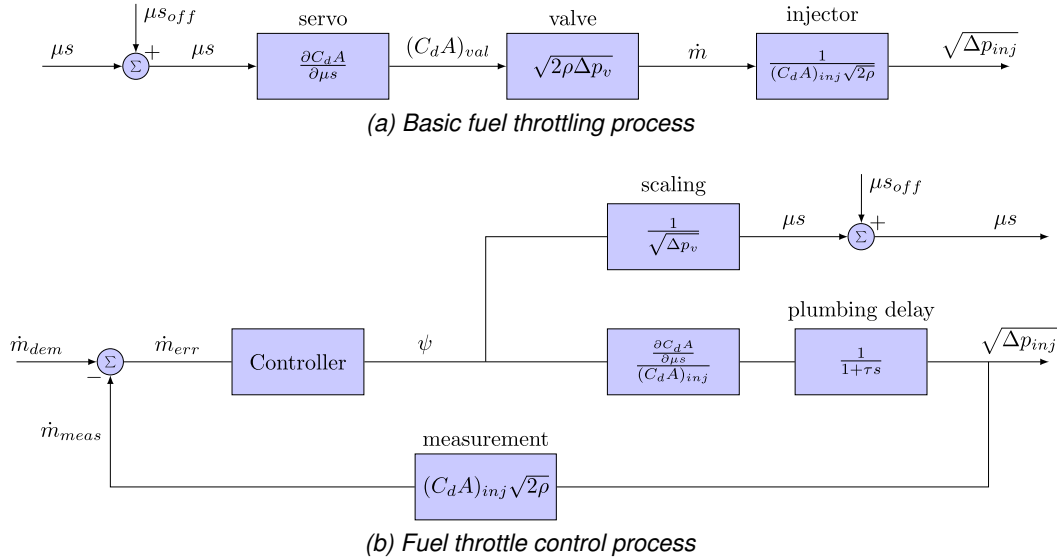


Figure 6: Block diagram of the fuel throttle process (a), and control system (b). The initial thruster model used a simplistic low-pass filter model of the IPA injector to model the ‘delay’ due to filling the plumbing volume.

and their discharge coefficient, $C_d A_{inj}$, can be found by calibration then the injectors themselves can be used to estimate the IPA massflow. Alternatively, the IPA massflow could be estimated by calibrating pressure drop against massflow for the throttle valve, and the pressure drop across the throttle valve could be used as a feedback parameter. This method is more complicated, however, because the valve flow area varies whereas the injector area is fixed, so this is not explored further in this paper.

The basic throttling process in Fig. 6a must be rearranged in order to provide a control process that can be implemented. Fig. 6b shows the fuel throttle control methodology. A desired IPA massflow is demanded, which passes through a controller which calculates an intermediate value, $\psi = \mu s \sqrt{\Delta p_v}$, where Δp_v is the pressure drop over the valve. This intermediate value is required so that the control loop can be designed using linear control system techniques, because it removes the nonlinear pressure drop relationship from the main loop. This intermediate variable can be scaled by the square root of the current pressure drop, and an estimated shutoff offset, μs_{off} , added to give the output pulse width to the servo drive.

A crude model of the thruster response is included for designing the IPA control loop, in order to capture the delay and low pass filter effect of the injector plumbing. Because IPA is incompressible, this effect is far less important than for the N_2O . A simple

low-pass filter is therefore used with time constant, τ , to design a proportional and integral controller. The physical time delay is neglected here; in the Laplace domain this would require a $e^{-s\tau}$ term, which is easy to specify but complex to truncate to a polynomial transfer function of finite length. Common approximations include Padé or Laguerre shifts [12].

The resulting closed loop step response is heavily damped and relatively insensitive to τ . Given that the thruster performance is fairly insensitive to mixture ratio, the simple IPA controller performance is considered sufficient for initial testing and no further system characterisation has been undertaken yet.

4.2. Nitrous oxide control system

The N_2O control system is fundamentally different to that of the IPA, in that it does not use a derived massflow value for feedback. This is because measuring the N_2O massflow accurately is difficult because it is multiphase. Given that the operating mixture ratio is 5.0, the N_2O oxide contributes the bulk of the massflow to the thruster. The N_2O control system therefore uses feedback directly from the chamber pressure, with the assumption that the IPA control loop is performing correctly and therefore the mixture ratio will remain fairly constant.

Section 3 demonstrated that there is a roughly linear relationship between N_2O servo valve pulse width and chamber pressure (Fig. 4). Fig. 7 shows the

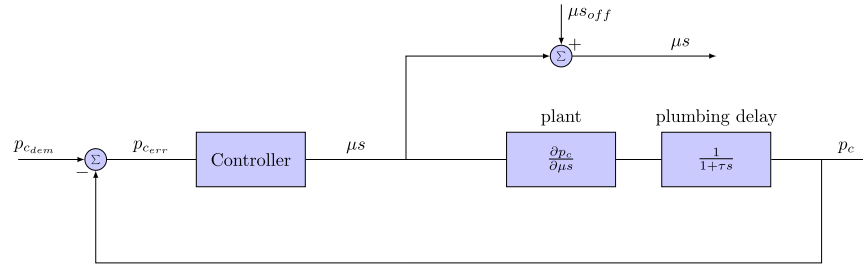


Figure 7: N_2O throttle control system methodology. The chamber pressure is used as the demand and feedback variable. An initial thruster model of a low pass filter is shown here, which was later replaced by an experimentally derived transfer function.

N_2O control system methodology. The initial model for the plumbing delay is a low pass filter, where the time constant, τ , is taken to be 0.2s. This value comes from a fit to the leading edge of the steps in Fig. 3. A proportional-integral controller was designed based on this control methodology.

4.2.1. Thruster model fitting

Once initial control systems had been designed, it was possible to perform closed loop throttle testing and test the step response of the system. Using the data from these tests, a second order transfer function was fitted to this data to improve the thruster model from the simple low-pass filter assumption.

For the step response of a second order damped system, the overshoot and damped natural frequency, ω_d , can be related to the peak overshoot, M_{pk} , and the damping ratio, ζ [13]. The peak (pk) overshoot is related to the damping ratio, ζ , and steady state (ss) value by:

$$M_{pk} = \frac{y_{pk} - y_{ss}}{y_{ss}} = e^{\frac{-\pi\zeta}{\sqrt{1-\zeta^2}}} \quad (8)$$

which can be rearranged to:

$$\zeta = \sqrt{\frac{\ln^2 M_{pk}}{\ln^2 M_{pk} + \pi^2}} \quad (9)$$

From the step response the natural frequency (undamped) can be estimated from the damped natural frequency by:

$$\omega_n = \frac{\omega_d}{\sqrt{1-\zeta^2}} \quad (10)$$

A second order damped system has the transfer function:

$$M(s) = \frac{\omega_n^2}{s^2 + 2\zeta\omega_n s + \omega_n^2} \quad (11)$$

In the case of the static test data from a closed-loop test, this transfer function represents the closed-loop product of the controller and thruster. If the controller has transfer function $G(s)$ and the thruster has transfer function $H(s)$, then:

$$M(s) = \frac{G(s)H(s)}{1 + G(s)H(s)} \quad (12)$$

The natural frequency of the thruster system was estimated to be 0.75Hz with damping ratio of 0.36. The frequency was lower than anticipated, possibly because there is a hose between the throttle valve and injector for mechanical reasons, and therefore a time delay due to filling/venting the plumbing volume. This volume will be reduced during future testing.

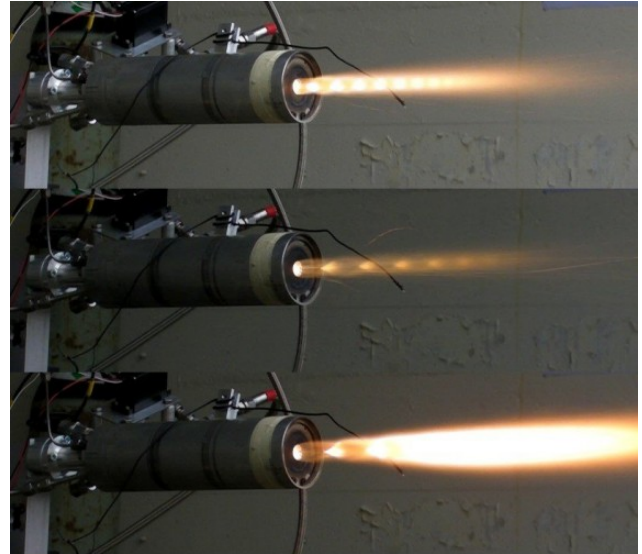
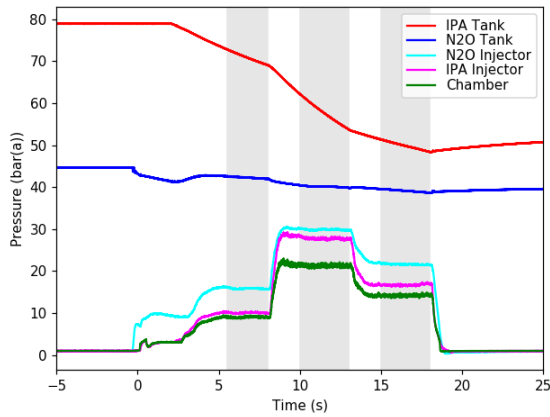
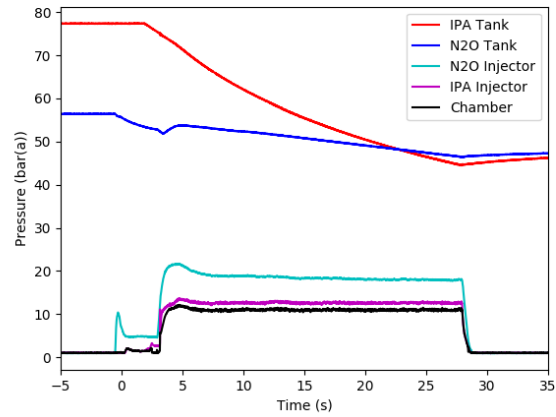


Figure 8: Throttle testing of the Snark bipropellant thruster. The black wire is a pyrotechnic igniter.



(a) Multiple short throttle steps



(b) One long step at 11.0bar(a)

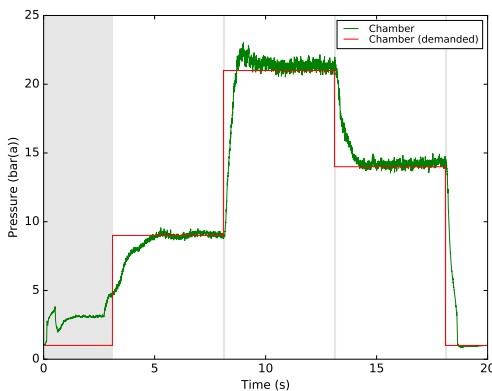
Figure 9: Pressures from closed loop testing. Time-averaging windows are shown as vertical gray bars in (a).

5. RESULTS

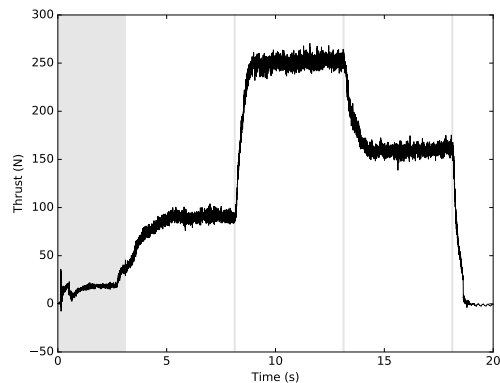
The Snark thruster has been static tested successfully at a range of throttle levels. Fig. 8 shows images from a horizontal static test at three different throttle levels. Figs. 9a and 10 shows the thruster response to a multiple step throttle test, and Fig. 9b shows the thruster response to a long test at constant chamber pressure. In both cases the desired chamber pressure is maintained well despite large decreases in the tank pressures.

Fig. 10 shows several important features. First, that the response to the first throttle step was slower than the rest. The thruster warm-up sequence was adjusted and shows better performance in the long test

(Fig. 9b). Second, that the thrust profile is smooth and is maintained well. The thrust profile does not show an overshoot when stepping up in thrust, but the chamber pressure does show an overshoot. Given that this is replicated on a second chamber pressure sensor (not shown) and the IPA injector pressure, this seems to be a physical effect. Third, that the response to a throttle position change takes just over a second; this is also true for shutdown. This is acceptable for the initial round of vehicle testing but could be improved. Future tests will attempt to reduce the plumbing volume downstream of the throttle valves, before re-characterising the thruster from experimental data and re-designing the control loops.



(a) Chamber pressure



(b) Thrust

Figure 10: Closed loop throttle testing, showing the demanded and achieved chamber pressure and the resulting thrust. The wide, vertical gray bar indicates the ignition and warm up sequence, the gray lines indicate switching between throttling steps.

6. CONCLUSIONS

The Gyroc 5 VTVL vehicle has a N_2O / IPA thruster, fed by a self-pressurising tank of N_2O and a blowdown tank of IPA. The vehicle must be able to throttle the thruster quickly and accurately in order to have the desired flight dynamics. Throttling the IPA is difficult because the upstream tank pressure is decreasing quickly, but throttling the N_2O is more difficult because the flow through the throttle valve and injectors is two phase.

During static testing, two key points were noted: first, that the N_2O injector pressure drop into the combustion chamber was found to be almost independent of massflow, because of a balance between flash-boiling in the control valve and flash-boiling in the injectors, and second, that the chamber pressure varied almost linearly with the pulse width provided to the N_2O servo control valve. The N_2O throttle control system is therefore designed to use feedback control from the combustion chamber pressure, based on a second order transfer function of the thruster response derived from experimental data. The IPA throttle control system uses feedback from the injector pressure drop, which can be related to the massflow.

Data is presented for several closed-loop throttle tests. The control loops have been demonstrated to throttle the thruster well enough to proceed to initial vehicle flight testing.

REFERENCES

- [1] Devolites, J. & Hart, J., (2014). Morpheus Vertical Test Bed Flight Testing. *2014 IEEE Aerospace Conference*, Big Sky, MT, US.
- [2] Olansen J., Munday, S. & Mitchell J. (2013). Project Morpheus: Lessons Learned in Lander Technology Development. *AIAA Space 2013 Conference*, San Diego, CA, US.
- [3] Paschall, S. & Brady, T., (2014). Rocket validation of the ALHAT autonomous GNC flight system. *2014 IEEE Aerospace Conference*, Big Sky, MT, US.
- [4] Waugh, I., Davies, A., Moore, E. and Macfarlane, J. (2016). VTVL technology demonstrator vehicle for planetary landers, *Space Propulsion Conference*, Rome.
- [5] Waxman, B., et al. (2013). Mass flow rate and isolation characteristics of injectors for use with self-pressurizing oxidizers in hybrid rockets, *49th AIAA/ASME/SAE/ASEE Joint Propulsion Conference*, San Jose, CA.
- [6] Dyer, J., et al. (2007). Modeling Feed System Flow Physics for Self-Pressurizing Propellants, *43rd AIAA/ASME/SAE/ASEE Joint Propulsion Conference and Exhibit*, Cincinnati, OH.
- [7] Solomon, B. (2011). Engineering Model to Calculate Mass Flow Rate of a Two-Phase Saturated Fluid Through An Injector Orifice, Utah State University.
- [8] Peterson, Z. (2012). Closed-loop thrust and pressure profile throttling of a nitrous oxide/hydroxyl-terminated polybutadiene hybrid rocket motor, Utah State University, US
- [9] Whitmore, S., Peterson, Z. & Eilers, S. (2014). Closed-loop precision throttling of a hybrid rocket motor, *Journal of Propulsion and Power*, 30 (2)
- [10] Whitmore, S., Peterson, Z. & Eilers, S. (2014). Deep throttle of a nitrous oxide and hydroxyl-terminated polybutadiene hybrid rocket motor, *Journal of Propulsion and Power*, 30 (1)
- [11] McBride, B., & Gordon, S. (1996). Computer Program for Calculation of Complex Chemical Equilibrium Compositions and Applications, NASA RP1311.
- [12] Pekar, L. & Kureckova, E., (2011). Rational approximations for time-delay systems - Case studies. *13th WSEAS International Conference on Mathematical Methods and Techniques in Engineering and Environmental Science*.
- [13] Burns, R. (2001). *Advanced Control Engineering*, Butterworth-Heinemann, Oxford, UK.